Molecular Simulation of Displacement of Methane by Injection Gases in Shale

Jihong Shi[1,3], Liang Gong[1,*] , Zhaoqin Huang[2] and Jun Yao[2]
[1]College of Pipeline and Civil Engineering, China University of Petroleum (East China), Qingdao 266580, People's Republic of China
[2]School of Petroleum Engineering, China University of Petroleum (East China), Qingdao 266580, People's Republic of China
[3]Computational Transport Phenomena Laboratory, Division of Physical Science and Engineering, King Abdullah University of Science and Technology, Thuwal 23955-6900, Saudi Arabia
*Corresponding author E-mail:lgong@upc.edu.cn

Abstract. Displacement methane (CH_4) by injection gases is regarded as an effective way to exploit shale gas and sequestrate carbon dioxide (CO_2). In our work, the displacement of CH_4 by injection gases is studied by using the grand canonical Monte Carlo (GCMC) simulation. Then, we use molecular dynamics (MD) simulation to study the adsorption occurrence behavior of CH_4 in different pore size. This shale model is composed of organic and inorganic material, which is an original and comprehensive simplification for the real shale composition. The results show that both the displacement amount of CH_4 and sequestration amount of CO_2 see an upward trend with the increase of pore size. The CO_2 molecules can replace the adsorbed CH_4 from the adsorption sites directly. On the contrary, when N_2 molecules are injected into the slit pores, the partial pressure of CH_4 would decrease. With the increase of the pores width, the adsorption occurrence transfers from single adsorption layer to four adsorption layers. It is expected that our work can reveal the mechanisms of adsorption and displacement of shale gas, which could provide a guidance and reference for displacement exploitation of shale gas and sequestration of CO_2.

Keywords: Molecular simulation; Displacement of methane; shale gas; Injection gases.

1 Introduction

Recently, the exploration and development of shale gas have received extensive attention because of the demand for resources and pollution problems[1-3]. Shale gas has gained tremendous attention as an unconventional gas resource[4-5]. The main component of shale gas is CH_4, which has three states in shale, i.e., adsorbed state, free state and dissolved state[6-7]. The volume percentage of the adsorbed CH_4 in the shale reservoirs could even account for 20%~85%[8-9]. Therefore, it is significant to investigate the adsorbed CH_4 in shale reservoirs for shale gas resource evaluation.

ICCS Camera Ready Version 2018
To cite this paper please use the final published version:
DOI: 10.1007/978-3-319-93713-7_11

Exploration shale gas become very difficult due to the ultralow porosity and permeability shale. Right now, many methods are proposed to boost production of shale gas, for example, re-fracturing, hydro-fracturing, supercritical CO_2 fracturing, injection gases, etc. Hydro-fracturing, as a method of widely application, is used to enhance permeability of unconventional reservoirs[10-12]. Moreover, this method could waste large amount of water and cause severe environment problems[13-15]. Alternatively, the new method of injection gases is regarded as a good way to improve the recovery efficiency[16-18]. Meanwhile, shale gases are usually stored as adsorption state in silt pore and carbon nanotube. Therefore, investigations about the displacement and diffusion of methane in silt pores are of great significance for estimating and exploiting the shale gas.

Extensive computational studies and experiments on the displacement of CH_4 in shale matrix reported at present. Yang[18] investigated competitive adsorption between CO_2 and CH_4 in Na-montmorillonites by Monto Carlo simulations, and found that the Na-montmorillonite clay shows obviously high adsorption capacity for CO_2, as compared with CH_4. Wu[16] explored the displacement of CH_4 in carbon nanochannels by using molecular dynamics simulations, and found that CO_2 can displace the adsorbed CH_4 directly. Akbarzadeh[19] also performed MD simulations on the mixture of shale gas (methane, ethane and propone) in a nanoscale pore graphite model, and found that the most selectivity (and also recovery) of methane obtains at the methane mole fraction of 0.95. Huo[20] conducted experiments to study the displacement behaviors of CH_4 adsorbed on shales by CO_2 injection, and found that the amount of recovered CH_4 and stored CO_2 increase with CO_2 injection pressure. Huang[21] investigated the adsorption capacities of CH_4, CO_2 and their mixtures on four kerogen models with different maturities by GCMC simulations. And they found that the adsorption capacity of gas molecules is related to the maturity of kerogen.

From the studies mentioned above, most of the shale models are nanosized and simplified. Because some free gases would occupy large pores and adsorbed gases would exist in organic matter and inorganic minerals. For the shale matrix, it is indispensable to simplify the complicated structure of shale matrix to deal with the complex situation. Someone argued that the structure of montmorillonite with some ions could represent the shale. However, this model still did not include the organic matter. At last, it is reasonable and appropriate to construct an all-atom shale model including inorganic silica and organic matter to investigate the displacement and diffusion of CH_4 in gas shale matrix.

In this work, we proposed a modified and generalized shale matrix model including inorganic silica and organic matter. Then, the mechanism of the displacement of CH_4 by injection gases in shale matrix model was investigated through molecular simulations. Finally, some discussion was also addressed. In section 3.1, the occurrence behaviors of CH_4 in different pore size are found to become from one adsorption peak to four adsorption peaks. In section 3.2, CO_2 is injected into shale model to displace the adsorbed CH_4. The displacement efficiency and sequestration amount of CO_2 are investigated. In section 3.3, the displacement CH_4 by CO_2 and N_2 are compared and analyzed.

ICCS Camera Ready Version 2018
To cite this paper please use the final published version:
DOI: 10.1007/978-3-319-93713-7_11

2 Simulation models and methods

2.1 Shale models

In order to construct the shale model containing inorganic minerals and organic matter, two silica sheets are used to stand for the inorganic mineral. Because the silica's brittleness is favorable for fracture propagation. We can get the initial silica lattice from the structure database of Material Studio software[22]. Along the (1 1 0) crystallographic orientation, we can cleave a repeat unit with the thickness 3.0 nm. Generally, the polycyclic aromatic hydrocarbon is regarded as the major organic component of organic matters, especially for shale gas reservoirs. Therefore, we used methylnaphthalene molecules to stand for the organic matter in the shale matrix here.

A simulation box was constructed to (32.43 × 39.30 × c $Å^3$), which contains two inorganic layers and two organic layers (see Fig. 1). As mentioned above, the perfect silica sheets were used to represent the inorganic layers. First, two perfect silica sheets were stacked each other in such a way as shown in Fig. 1. Then, methylnaphthalene molecules were absorbed into the interlayer space. The adsorbed methylnaphthalene molecules in slit pores were fixed[23].

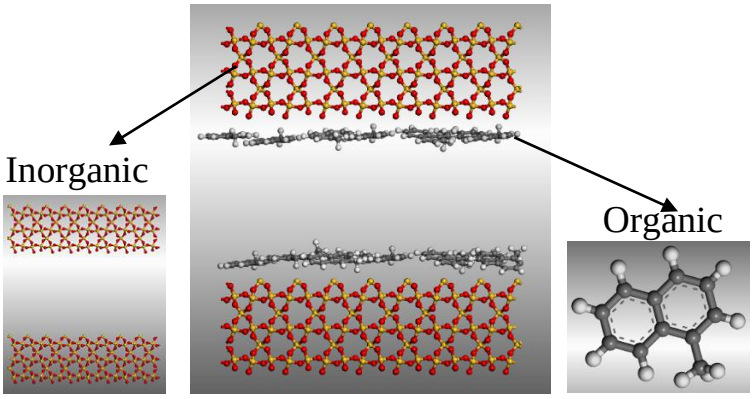

Fig. 1. The model of shale matrix. Color scheme: yellow, silicon; red, oxygen; white, hydrogen; black, carbon.

2.2 Methods

GCMC simulations are carried out by SORPTION code in the MATERIAL STUDIO (MS) software developed by Accelrys Inc. The interatomic interactions are described by the force field of condensed-phase optimized molecular potential for atomistic simulation studies (COMPASS), which is a general all-atom force field. First, we took the GCMC method to investigate the displacement of CH_4 by CO_2. The temperature and the pressure of CH_4 were 313 K and 15 MPa respectively. The acceptance or rejection of trial move is set as the Metropolis algorithm. Each equilibration procedure for CO_2 and CH_4 is 2×10^6. Next, CO_2 was put into the slit pores with injection pressure from

ICCS Camera Ready Version 2018
To cite this paper please use the final published version:
DOI: 10.1007/978-3-319-93713-7_11

0 to 110 MPa. We could get the equalized structure until the process of simulation was ended.

In order to adjust the atomic coordinates to reach a stable initial configuration, the equalized structure was minimized by using the conjugate gradient algorithm. Then, we took MD method to study the density profile of adsorbed CH_4. First, the model was relaxed for 2 ns in a NVT ensemble with a time step of 1 fs. The Nose-Hoover thermostat method was used to maintain temperature. When we found that total energy of this model became time-independent, the equilibrium was arrived. In the last stage, this system experienced a simulation process of 2 ns in a NVE ensemble (constant number of atoms, isovolumetric, and constant energy conditions) with a time step of 1fs, and the data were recorded for analysis. During these simulations, all the atoms of the shale matrix model were fixed as a rigid material.

3 Results and discussion

3.1 Occurrence behavior of methane in different pores

The occurrence behaviors of methane in different pores are absolutely different, which is a significant aspect to reveal the adsorption behaviors of methane in shale. In this section, a series of shale model of different size pores from 10 Å to 100 Å are built. All of these shale models have undergone GCMC process to achieve the equilibrium state of adsorption, before they are subjected to MD simulations. Then, we can get some data about the density profile of CH_4 in pores. Fig. 2.shows the different density profiles.

A single adsorption peak is founded in Fig. 2a. The distance between two solid walls of 10 Å is very close, the attractive potentials of two walls are strengthened by each other. A large amount of CH_4 would accumulate in the central of the pore. The peak of adsorption layer is the second highest at 0.65 $g{\cdot}cm^{-3}$, compare with 0.75 $g{\cdot}cm^{-3}$ at 15 Å. Since the pore size is the narrowest in all cases, the amount of adsorption methane is limited. A small amount of methane molecules absorbed in the pore, which results in the peak of adsorption layer is not the highest. As the size of pore increases, the single adsorption layer would become two adsorption layers. The attractive potentials of two walls become weak or even disappear. Meanwhile, the peaks of adsorption layer are the highest. It can be seen from the Fig. 2b. When the distance of two walls increases to 25 Å, apart from two peaks, a central single layer appears. Two peaks near the walls

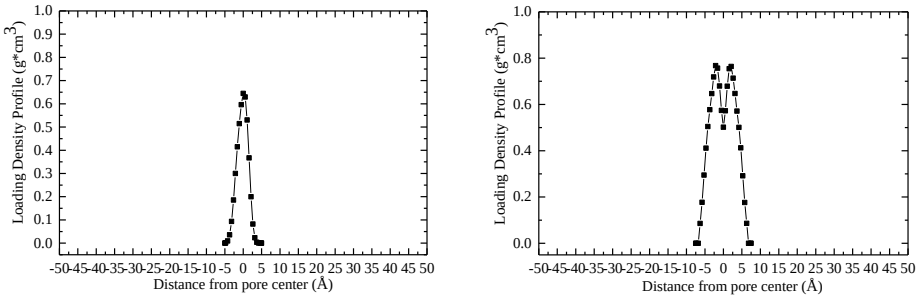

(a) H=10 Å (b) H=15 Å

ICCS Camera Ready Version 2018
To cite this paper please use the final published version:
DOI: 10.1007/978-3-319-93713-7_11

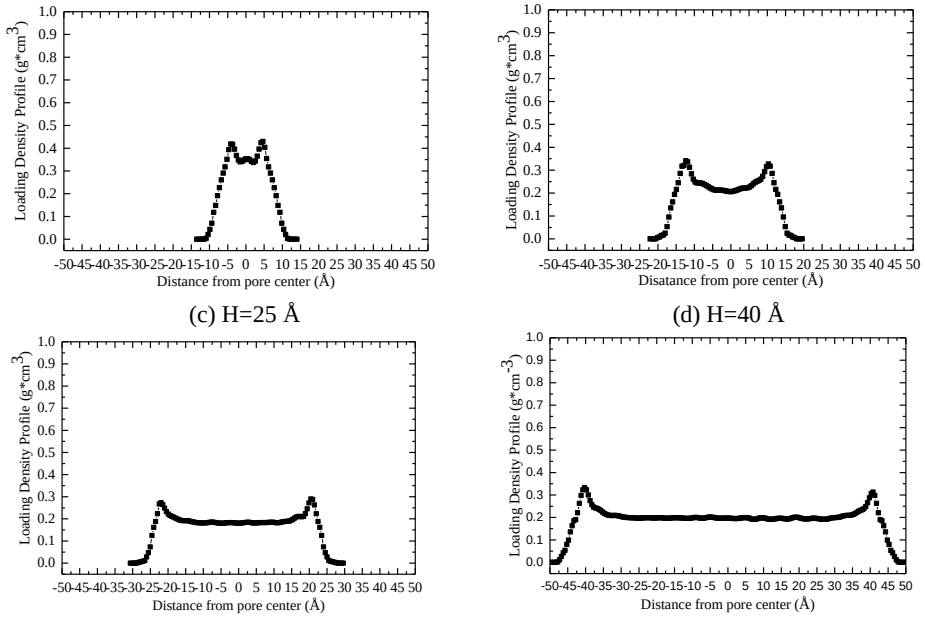

Fig. 2. Loading density profile and adsorption state of methane in different pores. (a) H=10 Å, single adsorption layer; (b) H=15 Å, two adsorption layers; (c) H=25 Å, two adsorption layers and central single layer; (d) H=40 Å, two adsorption layers and two secondary layers; (e) H=60 Å, two adsorption layers and middle bulk phase; (f) H=100 Å, two adsorption layers and middle bulk phase.

are lower, around half the figure for H=15 Å. Four peaks of adsorption layers, including two primary adsorption layers and two secondary, will appear at 40 Å[17]. Fig. 2e and Fig. 2f show that the density of bulk phase is all keep in at 0.2 $g \cdot cm^{-3}$ at the pore width of 60 ~ 100 Å. This situation illustrates that the central bulk phase will not change with the silt width increases.

In order to show the state of molecular occurrence more intuitively, we give snapshots of the adsorption model in two pore sizes. The pore sizes are set as 25 Å and 60 Å, representing mesopores and macropores respectively. Fig. 3a shows that the amount of adsorbed CH_4 next to the walls is much more than the bulk's. So near the walls, two symmetrical peaks appeared. However, the center of the pore is still adsorbed with a certain amount of CH_4. Correspondingly, a small peak appears in the center of the density profile graph. In contrast to, when the pores become macropores, no more peaks appear in the center of the pores. It can be seen from Fig. 3b. Because in the case of large pore, the density of methane in the central area basically does not change.

ICCS Camera Ready Version 2018
To cite this paper please use the final published version:
DOI: 10.1007/978-3-319-93713-7_11

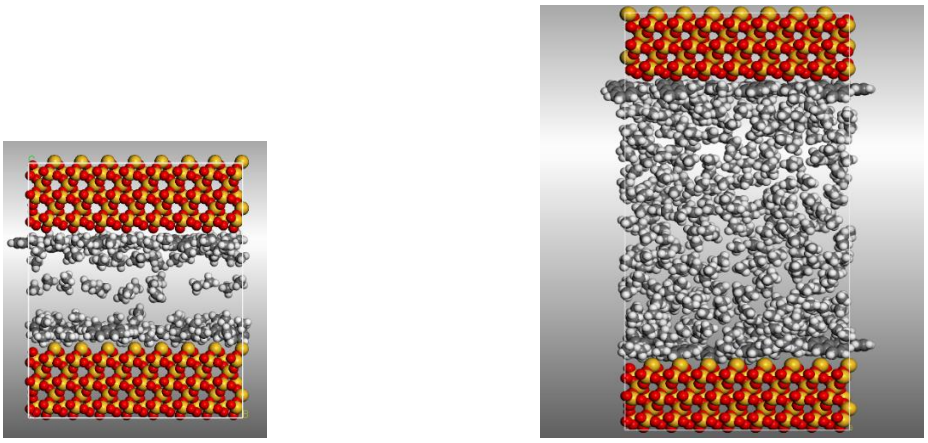

(a) 25 Å (b) 60 Å

Fig. 3. Adsorption occurrence of CH4 in different pores.

3.2 Methane displacement by carbon dioxide in different pores

Injection gases has become a high efficient way to exploit the shale gas. CO_2 and N_2 are usually considered ideal gases to displace methane. Some studies find that the adsorption capacity of gases is related to the attractive potentials between gases and shale matrix atoms. Fig. 4a shows the changes of loading amount of CH_4 at different CO_2 injection pressure in different pores. The size of pore is set 15~100 Å. Obviously, the downward trend in loading amount of CH_4 is significant at different pores. As the injection pressure of CO_2 increases, the loading amount of CH_4 in the shale model diminishes. For injection pressure of 0~30 MPa, the loading amount of CH_4 decreases quickly. When CO_2 is injected, the molecules can adsorb on the walls to replace the adsorbed methane. At high pressure, there are no more adsorption sites for CO_2 molecules to adsorb. The curve becomes smooth at high CO_2 injection pressure. The loading amount of CH_4 starts to stay stable. With the increase of the pores width, the loading amount of CH_4 at different CO_2 injection pressure increases obviously. Similarly, the sequestration amount of CO_2 rises significantly. For the same width of pore, the figure for sequestration CO_2 grows dramatically, which is shown in the Fig. 4b. Furthermore, the displacement amount of CH_4 at CO_2 injection pressure of 90 MPa is studied. Much more CO_2 is absorbed into the pores with the increase of pore width, causing more methane to be driven out. So Fig. 4c shows that the displacement amount of CH_4 is the highest in the pore size of 100 Å. Correspondingly, the sequestration amount of CO_2 is also the most. It can be seen from Fig. 4d.

ICCS Camera Ready Version 2018
To cite this paper please use the final published version:
DOI: 10.1007/978-3-319-93713-7_11

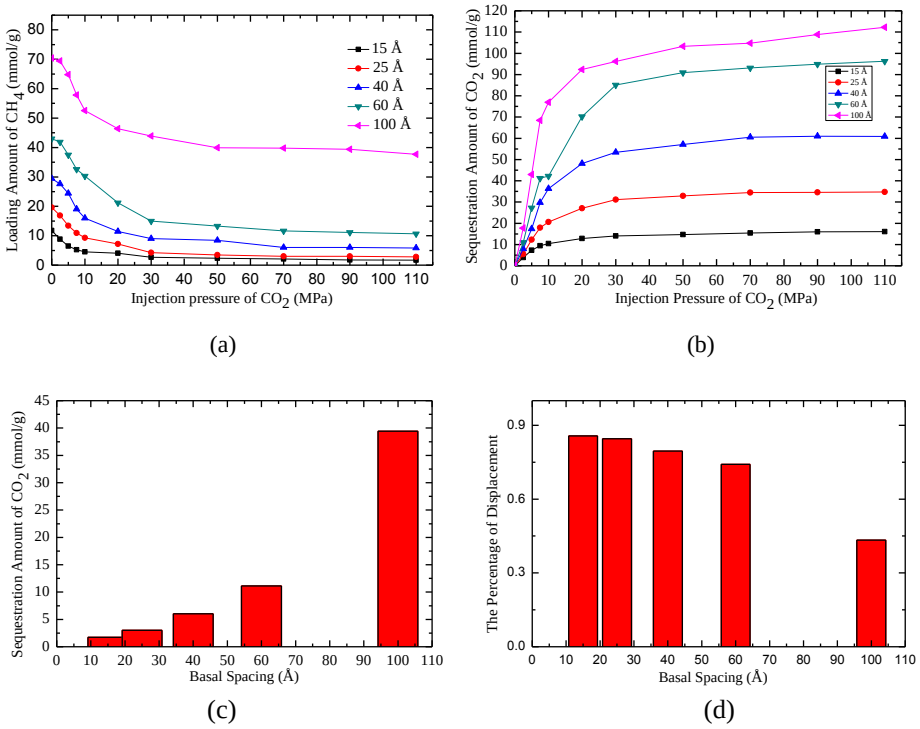

Fig. 4. Displacement of methane by carbon dioxide in different pores. (T_m=313 K, P_m=15 MPa) (a) Loading amount of CH_4 at different CO_2 injection pressure; (b) Sequestration amount of CO_2 at different CO_2 injection pressure; (c) Displacement amount of CH_4 at CO_2 injection pressure of 90 MPa; (d) Sequestration amount of CO_2 at CO_2 injection pressure of 90 MPa.

3.3 Comparison of methane displacement by nitrogen and carbon dioxide

Both N_2 and CO_2 can be used to displace gases. However, our studies find that the displacement mechanisms of these gases is different. The pore width is set 25 Å. Fig. 5 shows the difference between these two gases. Fig. 5a shows the loading amount of CH_4 at different injection pressure. In the case of CO_2 displacing CH_4, the loading amount of methane decreases significantly as the partial pressure of CO_2 increases, compared with the case of N_2 displacing CH_4. Both kinds of gases displacement have led to a sharp decline in loading amount of CH_4. Correspondingly, the sequestration amount of CO_2 has also increased rapidly in the cases of the displacement of methane by CO_2 and N_2. More CO_2 will displace the methane to concentrate in the adsorbed layer, and N_2 will displace less. When CO_2 is added into the pores, the full of this space is filled with CO_2 molecules. Then, CO_2 molecules begin to occupy adsorption sites of CH_4, replacing the adsorbed CH_4 molecules directly. The displaced CH_4 molecules return to free phase. The adsorption capacity of these three gases is sorted as follows:

ICCS Camera Ready Version 2018
To cite this paper please use the final published version:
DOI: 10.1007/978-3-319-93713-7_11

CO_2 > CH_4 > N_2. In contrast to, when N_2 is injected, N_2 molecules cannot occupy adsorption sites of CH_4. These N_2 molecules can only adsorb on the vacancies due to the fact that the adsorption capacity of N_2 is weaker than CH_4. N_2 molecules are able to displace CH_4 because they can reduce the partial pressure of CH_4. Once the partial pressure of CH_4 decreases, CH_4 molecules would be desorbed and displaced. Therefore, as CO_2 and N_2 are injected, the loading amount of methane all experiences a downward trend. . The screenshots of different displacement processes is shown in Fig. 6.

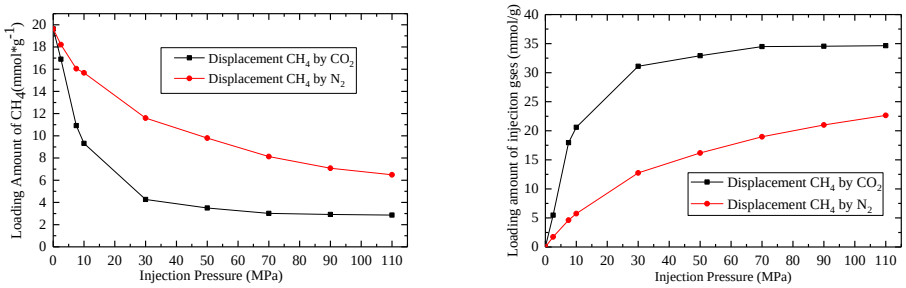

(a) (b)

Fig. 5. Comparison of methane displacement by CO_2 and N_2. (T_m=313 K, P_m=15 MPa, H=25 Å) (a) Loading amount of CH_4 at different injection pressure; (b) Sequestration amount of injection gases at different injection pressure.

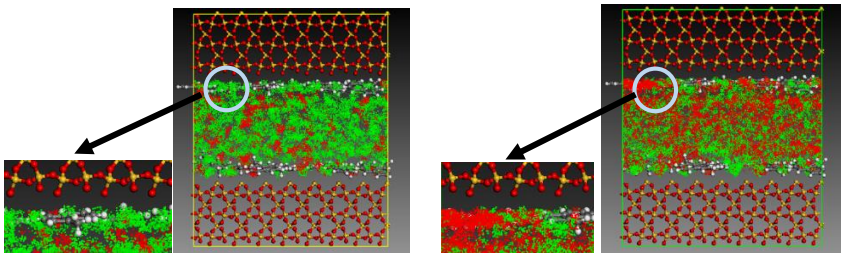

(a) CO_2 (b) N_2

Fig. 6. The adsorption sites snapshots of displacement of CH_4. (P_I=90 MPa) (a) Displacement of CH_4 by CO_2: red-CH_4; green-CO_2. (b) Displacement of CH_4 by N_2: red-CH_4; green-N_2

4 Conclusion

On the basis of adsorption characteristics of CH_4 on the shale model, we built a new shale model by using organic-inorganic composites. Then we used GCMC simulation to study the displacement of shale gas by CO_2 and N_2. The displacement mechanisms of the injection gases are investigated. Next, the occurrence behavior of methane in different pores is investigated by using the MD method. Our conclusions are listed as follows:

ICCS Camera Ready Version 2018
To cite this paper please use the final published version:
DOI: 10.1007/978-3-319-93713-7_11

1. With the pores width increase, the adsorption occurrence transfers from single adsorption layer to four adsorption layers. In the case of a much wide pore width, the density of the central bulk phase approaches to the same value at 0.2 $g \cdot cm^{-3}$.
2. To displace the adsorbed CH_4, CO_2 and N_2 are injected and investigated. The results indicate that both of the CO_2 and N_2 molecules can displace the adsorbed shale gas and CO_2 is sequestrated into the shale simultaneously.
3. However, the displacement mechanisms of the injection gases are different. The adsorption capacity of CO_2 is much stronger than that of CH_4. The CO_2 molecules can replace the adsorbed CH_4 from the adsorption sites directly. On the contrary, when the pores are occupied by N_2 molecules, these molecules can decrease the partial pressure of CH_4.

It is expected these results and findings are of great importance for displacement exploitation of shale gas and sequestration of CO_2.

Acknowledgements

This study was supported by the National Natural Science Foundation of China (No. 51676208) and the Fundamental Research Funds for the Central Universities (No. 18CX07012A).

References

1. Arora V, Cai Y. US natural gas exports and their global impacts[J]. Applied Energy, 2014, 120: 95-103.
2. Howarth R W, Santoro R, Ingraffea A. Methane and the greenhouse-gas footprint of natural gas from shale formations[J]. Climatic Change, 2011, 106(4): 679.
3. Li Y X, Nie H K, Long P Y. Development characteristics of organic-rich shale and strategic selection of shale gas exploration area in China[J]. Natural Gas Industry, 2009, 29(12): 115-118.
4. Bowker K A. Barnett shale gas production, Fort Worth Basin: Issues and discussion[J]. AAPG bulletin, 2007, 91(4): 523-533.
5. Caulton D R, Shepson P B, Santoro R L, et al. Toward a better understanding and quantification of methane emissions from shale gas development[J]. Proceedings of the National Academy of Sciences, 2014, 111(17): 6237-6242.
6. Howarth R W, Santoro R, Ingraffea A. Methane and the greenhouse-gas footprint of natural gas from shale formations[J]. Climatic Change, 2011, 106(4): 679.
7. Ji L, Zhang T, Milliken K L, et al. Experimental investigation of main controls to methane adsorption in clay-rich rocks[J]. Applied Geochemistry, 2012, 27(12): 2533-2545.
8. Johnson H E, Granick S. Exchange kinetics between the adsorbed state and free solution: poly (methyl methacrylate) in carbon tetrachloride[J]. Macromolecules, 1990, 23(13): 3367-3374.
9. Curtis J B. Fractured shale-gas systems[J]. AAPG bulletin, 2002, 86(11): 1921-1938.
10. Clark C, Burnham A, Harto C, et al. Hydraulic fracturing and shale gas production: technology, impacts, and policy[J]. Argonne National Laboratory, 2012.

ICCS Camera Ready Version 2018
To cite this paper please use the final published version:
DOI: 10.1007/978-3-319-93713-7_11

11. Clarkson C R, Haghshenas B, Ghanizadeh A, et al. Nanopores to megafractures: Current challenges and methods for shale gas reservoir and hydraulic fracture characterization[J]. Journal of Natural Gas Science and Engineering, 2016, 31: 612-657.
12. Chen H, Carter K E. Water usage for natural gas production through hydraulic fracturing in the United States from 2008 to 2014[J]. Journal of environmental management, 2016, 170: 152-159.
13. Jackson R E, Gorody A W, Mayer B, et al. Groundwater protection and unconventional gas extraction: the critical need for field‐based hydrogeological research[J]. Groundwater, 2013, 51(4): 488-510.
14. Connor J A, Molofsky L J, Richardson S D, et al. Environmental Issues and Answers Related to Shale Gas Development[C]//SPE Latin American and Caribbean Health, Safety, Environment and Sustainability Conference. Society of Petroleum Engineers, 2015.
15. Clarkson C R, Solano N, Bustin R M, et al. Pore structure characterization of North American shale gas reservoirs using USANS/SANS, gas adsorption, and mercury intrusion[J]. Fuel, 2013, 103: 606-616.
16. Wu H A, Chen J, Liu H. Molecular dynamics simulations about adsorption and displacement of methane in carbon nanochannels[J]. The Journal of Physical Chemistry C, 2015, 119(24): 13652-13657.
17. Yu H, Yuan J, Guo W, et al. A preliminary laboratory experiment on coalbed methane displacement with carbon dioxide injection[J]. International Journal of Coal Geology, 2008, 73(2): 156-166.
18. Yang N, Liu S, Yang X. Molecular simulation of preferential adsorption of CO 2 over CH 4 in Na-montmorillonite clay material[J]. Applied Surface Science, 2015, 356: 1262-1271.
19. Akbarzadeh H, Abbaspour M, Salemi S, et al. Injection of mixture of shale gases in a nanoscale pore of graphite and their displacement by CO2/N2 gases using molecular dynamics study[J]. Journal of Molecular Liquids, 2017, 248: 439-446.
20. Huo P, Zhang D, Yang Z, et al. CO 2 geological sequestration: Displacement behavior of shale gas methane by carbon dioxide injection[J]. International Journal of Greenhouse Gas Control, 2017, 66: 48-59.
21. Huang L, Ning Z, Wang Q, et al. Molecular simulation of adsorption behaviors of methane, carbon dioxide and their mixtures on kerogen: effect of kerogen maturity and moisture content[J]. Fuel, 2018, 211: 159-172.
22. Li X, Xue Q, Wu T, et al. Oil detachment from silica surface modified by carboxy groups in aqueous cetyltriethylammonium bromide solution[J]. Applied Surface Science, 2015, 353: 1103-1111.
23. Zhang H, Cao D. Molecular simulation of displacement of shale gas by carbon dioxide at different geological depths[J]. Chemical Engineering Science, 2016, 156: 121-127.

ICCS Camera Ready Version 2018
To cite this paper please use the final published version:
DOI: 10.1007/978-3-319-93713-7_11